PHILOSOPHICAL TRANSACTIONS OF THE ROYAL SOCIETY A MATHEMATICAL, PHYSICAL & ENGINEERING SCIENCES

Novel Meteorological Methods for Measuring Trace Gas Fluxes

O. T. Denmead

Phil. Trans. R. Soc. Lond. A 1995 **351**, 383-396
doi: 10.1098/rsta.1995.0041

Novel meteorological methods for measuring trace gas fluxes

By O. T. Denmead

CSIRO Centre for Environmental Mechanics, GPO Box 821, Canberra ACT 2601, Australia

The paper deals with flux measurements in two contexts: small plots and plant canopies. Mass balance methods have been developed for small experimental plots with lateral dimensions of tens of metres rather than the 1 m typical of chambers or the hundreds of metres required for conventional micrometeorological estimates. The general method relies on the conservation of mass to equate the differences in horizontal fluxes across upwind and downwind boundaries of a test plot with the surface flux within the plot along the line of the wind. Applications to soil and animal experiments are discussed.

Lagrangian descriptions of transport now supplant older, but inappropriate gradient-diffusion theory for inferring fluxes and source–sink distributions of scalars in plant canopies. An inverse Lagrangian theory due to M. R. Raupach provides a relatively simple observational and computational scheme for making such inferences from measurements of mean concentration profiles and canopy turbulence. The scheme and a range of applications are described.

1. Introduction

The methods commonly used for measuring trace gas fluxes are appropriate on either the microscale (chambers with length scales of order 1 m) or the macroscale (conventional micrometeorological techniques requiring fetches of hundreds of metres to kilometres). The notoriously large point-to-point variability of trace gas emissions necessitates extensive replication of chamber measurements or the use of larger space scales. Conventional micrometeorological methods, based on gradient diffusion, eddy correlation or eddy accumulation, fill the latter need, but require large, flat, uniform sites – usually difficult to find. Further, if the trace gas is produced as a result of an imposed surface treatment, application over a large area is likely to be expensive and time-consuming. The time course of gas emission immediately after the treatment is imposed may, however, be a desired experimental result. Liberation of ammonia or pesticides from soil applications are two such examples. There is then a place for techniques appropriate to intermediate space scales, requiring test plots of, say, tens of metres in lateral extent.

Small-plot meteorological techniques have been in existence for a considerable time, but the last decade has seen them used extensively for trace gas flux measurement. Based on mass balance, the general method equates the differences in horizontal gas fluxes across the upwind and downwind boundaries of a test plot with the surface flux of the gas within the plot along the line of the wind. Ap-

Phil. Trans. R. Soc. Lond. A (1995) **351**, 383–396
Printed in Great Britain

plications to measurement of trace gas fluxes from strips, circles and rectilinear plots and from plane and point sources are described here.

While the net flux of a trace gas between surface and atmosphere may be sufficient information in studies of atmospheric pollution or the compilation of trace gas inventories, knowledge of the sources and sinks of trace gases within the soil–plant system may be required for understanding at the process level. A simple example is CO_2 assimilation by plants in the field where both atmosphere and soil contribute. Early attempts at flux measurement within plant canopies relied on gradient-diffusion approaches, but it is now apparent that this approach is inappropriate in the canopy space (Finnigan 1979; Shaw *et al.* 1983; Denmead & Bradley 1985, 1987; Raupach *et al.* 1986). Most of the transport occurs in short, infrequent bursts when very large eddies penetrate downwards into the canopy space. In these circumstances, mean concentration profiles provide inaccurate and often misleading pictures of canopy transport. Apparent counter-gradient or zero-gradient fluxes in the canopy space are common. The mean concentration profiles reflect more the distribution of sources and sinks than the direction of scalar transport.

Alternative approaches to canopy transport have been developed in consequence, e.g. higher order closure models (Wilson & Shaw 1977; Finnigan & Raupach 1987), large-eddy simulation (Shaw & Schumann 1992), wavelet analysis (Collineau & Brunet 1993) and Lagrangian dispersion models (Raupach 1989*a–c*; Raupach *et al.* 1992). This paper concentrates on Lagrangian dispersion, which treats the canopy as an assembly of source elements, each releasing a plume of scalar material into the turbulent air flow within and above the canopy. The behaviour of the plumes near and far from the source elements accounts for the shapes of the mean concentration profiles developed in canopies and phenomena such as the apparent counter-gradient flows mentioned above. Application of the Lagrangian approach to the inverse problem of inferring source–sink distributions from the mean concentration profiles, first mooted by Raupach (1989*c*) in a Discussion Meeting of the Royal Society six years ago, has been a very significant recent development, providing a new way to calculate source strengths of scalars within the canopy from relatively simple measurement and computational schemes (Raupach *et al.* 1992; Denmead & Raupach 1993). Applications to flux inference in crops of wheat and sugar cane are described here.

As indicated above, the emphasis of this paper is on application rather than theory. Brief theoretical backgrounds are given for each of the methodologies described. More detailed explanations of theory are contained in several of the publications referred to.

2. Mass balance methods

Gases emitted from the ground spread vertically by turbulent diffusion and are convected horizontally by the wind. Footprint analyses (e.g. Leclerc & Thurtell 1990) indicate that for neutral conditions and surfaces with roughnesses typical of short crops and grasslands, more than 90% of the emitted gas is contained within a cloud which extends to a height Z of about 1/10 of the fetch X. In unstable conditions, the height of the cloud will be greater and in stable conditions, smaller. Figure 1 from Denmead (1983) illustrates these points. It shows profiles of atmospheric ammonia concentration on the downwind edge of a 30 m wide plot fertilized with urea, for three stability conditions. (The ammonia is formed

PHILOSOPHICAL TRANSACTIONS OF THE ROYAL SOCIETY A MATHEMATICAL, PHYSICAL & ENGINEERING SCIENCES

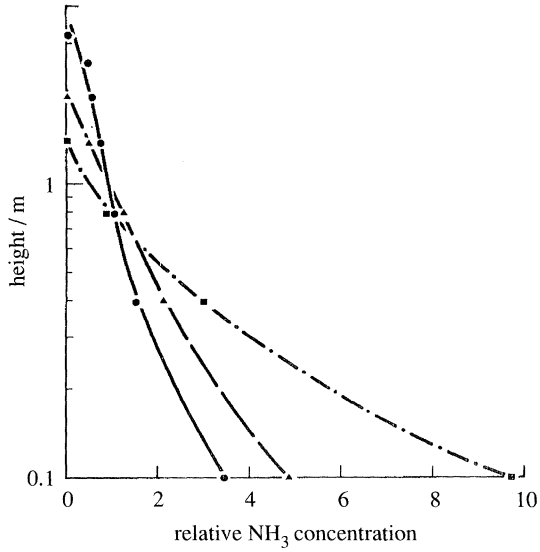

Figure 1. Influence of stability on shape of profiles of atmospheric ammonia concentration developed over urea-treated plots with fetch of 30 m. Abscissa is $\overline{\rho_g}/(\int_0^Z \overline{\rho_g}(z)\,dz/Z)$. L is the Monin–Obukhov length. ——, Unstable ($L = -3$ m); — —, neutral; — · —, stable ($L = 4$ m). (From Denmead 1983.)

through hydrolysis of the urea.) Stability is specified by the Monin–Obukhov length L. As stability varied from highly stable ($L = 4$ m) to highly unstable ($L = -3$ m), Z increased from 1.4 to 3.5 m.

The basic concept of the general mass balance method is simple. Consider a semi-infinite cross-wind strip, whose width along the line of the wind is X, emitting a gas whose atmospheric concentration on the downwind edge is ρ_g, a function of height z. Let the upwind, background concentration be ρ_b, which may also be a function of z. If the surface flux density of the gas is F, then from the conservation of mass,

$$F = \frac{1}{X}\int_0^Z \overline{U(\rho_g - \rho_b)}\,dz, \tag{2.1}$$

where $U(z)$ is the total horizontal wind speed, as measured by a cup anemometer, and the overbar denotes a time average.

A problem with the practical application of (2.1) is that the term is the mean of instantaneous fluxes. Writing U, ρ_g and ρ_b as the sums of means $\overline{U}$, $\overline{\rho_g}$ and $\overline{\rho_b}$ and fluctuations about those means U', ρ_g' and ρ_b', equation (2.1) becomes

$$F = \frac{1}{X}\int_0^Z \left(\overline{U}\,\overline{\rho_g} - \overline{U}\,\overline{\rho_b} + U'\rho_g'\right)\,dz. \tag{2.2}$$

The first two terms in the integrand are the fluxes due to horizontal convection while the third represents a turbulent diffusive flux in the opposite (upwind) direction. The corresponding term in ρ_b' disappears because there is no horizontal gradient in ρ_b upwind. The first two terms, the products of the mean wind speed and the mean concentrations, are the ones usually measured. Field tests suggest that it might overestimate the true flux by about 15% (Leuning *et al.* 1985). Wind tunnel tests suggest 10% (Raupach & Legg 1984), while theoretical calculations

suggest up to 20% (Wilson & Shum 1992). An empirical correction of say, 15%, may suffice, although bigger corrections may be needed in very small plots and over very rough surfaces (Wilson & Shum 1992).

Passive samplers have been designed to measure the instantaneous horizontal flux directly, thereby avoiding the problem just discussed. Passive samplers for ammonia have been described by Leuning *et al.* (1985) and Schoerring *et al.* (1992), but have not yet been devised for other gases. In what follows, it is assumed that the surface flux can be calculated (with a small correction) from profiles of mean horizontal windspeed and mean gas concentration on the upwind and downwind boundaries of the source plot. Unlike conventional micrometeorological methods, the aim is to measure concentrations right through the boundary layer developed over the plot rather than just in the shallow equilibrium layer close to the surface, which extends to a height of only about $X/100$. In this regard, the smaller the plot the better, whereas just the opposite holds for conventional methods. Typically, source plots have lateral dimensions of about 20 m.

Example applications of the method are given in figure 2 which shows profiles of $\overline{U}$, $(\overline{\rho_g}-\overline{\rho_b})$ and their product in three experiments concerned with emissions of ammonia following nitrogen fertilizer applications. The profiles over short grass have quite regular shapes and could be defined well enough by measurements at five levels. Profiles in the crop canopies, however, were irregularly shaped and required measurements at more levels to define them well enough for the integration in (2.2).

The need to work with differences between upwind and downwind concentrations can constitute a difficulty, not only because it entails extra measurement, but also because it involves the subtraction of experimentally determined data – an error-prone procedure. The technique is thus suited best to situations where ρ_b is small and experimental treatments generate fluxes that are large compared to normal emissions. One such situation where the method has been used extensively is measurement of ammonia emissions following application of nitrogen amendments to soils (see, for instance, Beauchamp *et al.* 1978; Denmead 1983; Ryden & McNeill 1984; Jarvis *et al.* 1989; Freney *et al.* 1992). Determining emissions from pesticide residues would be another highly appropriate application. Recently, the method has been used to measure emissions of nitrous oxide and methane during episodes of grazing (Jarvis 1990; Jarvis *et al.* 1993). Determination of methane production by cattle using a mass balance method is described later.

(*a*) *Plot shape*

Usually, agricultural experimenters work with rectilinear test plots in which fetch changes with wind direction. This necessitates careful and continuous measurement of wind direction and introduces uncertainty into the calculations when the direction changes significantly within a run. These problems are discussed by Ryden & McNeill (1984) for semi-infinite cross-wind strips and are considered in the context of square plots later in the paper. In the case of a plane source, the problem of changing fetch can be overcome by working with circular plots, and measuring U and ρ_g at their centre. Regardless of compass direction, the wind will always blow towards the centre and the fetch is always equal to the plot radius. For a circle, however, a further correction may be necessary to account for cross-wind diffusion, away from the plot centre. The calculations of Wilson & Shum (1992) suggest that this correction is small. Circular plot technology is

PHILOSOPHICAL TRANSACTIONS OF THE ROYAL SOCIETY A MATHEMATICAL, PHYSICAL & ENGINEERING SCIENCES

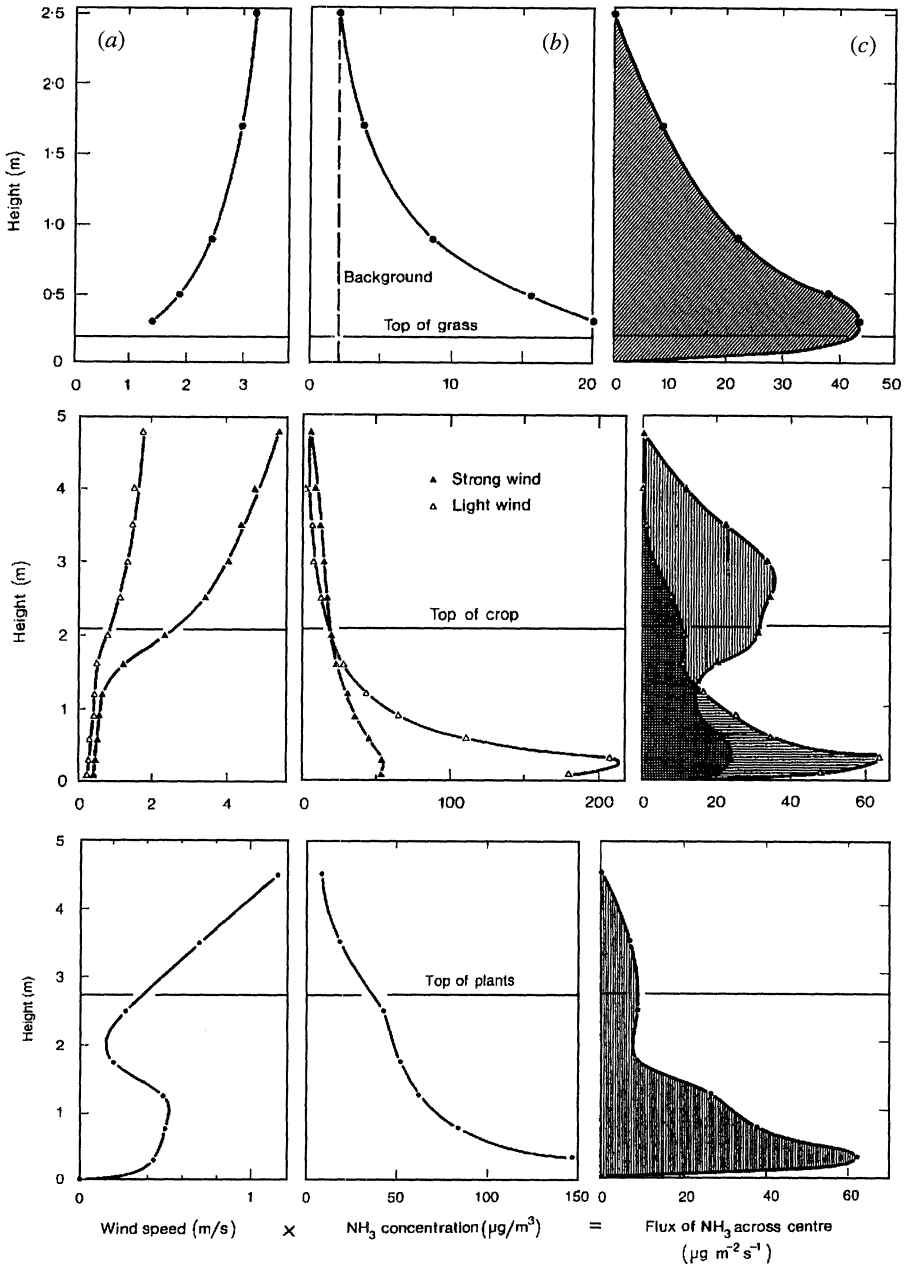

Figure 2. Application of the mass balance method showing mean wind speeds, ammonia concentrations and horizontal fluxes at the centres of treated plots emitting ammonia after application of urea fertilizer. Top for short grass, 0.2 m high, with a fetch of 25 m; centre for maize, 2.1 m high, with fetch of 35 m; bottom for banana plantation, 2.75 m high, with fetch of 15.5 m. (From Denmead 1994.)

now adopted widely (see, for instance, Beauchamp *et al.* 1978; Denmead 1983; Wilson *et al.* 1982, 1983; Wilson & Shum 1992).

(*b*) *Theoretical profile shape*

Both theory and experiment indicate that in some circumstances, it is possible to infer the surface flux from measurements of the horizontal flux at just one height. The main requirements are: (i) although the experimental plots should be small, the areas in which they are located should be large and uniform so as to ensure both horizontal equilibrium and predictable shapes for the wind and eddy diffusivity profiles; (ii) the treated area should have very short vegetation, if any, so that essentially all of the horizontal flux occurs in the unobstructed air layer above the surface; (iii) the surface emission should be driven by processes in the soil and/or vegetation rather than by the atmospheric gas concentration; i.e. there should be a constant flux rather than a constant concentration boundary condition at the surface.

In these circumstances, the profiles of concentration and horizontal flux density have a theoretically predictable shape that is determined by surface roughness, plot geometry and atmospheric stability (Wilson *et al.* 1982 and figure 1). From their analysis of the influence of stability on profile shape, based on a trajectory-simulation model, Wilson *et al.* (1982) predict the existence of a unique height within the plot boundary layer at which the normalized horizontal flux, $\overline{U}\overline{\rho_g}/F$, has almost the same value in all stability regimes. They designate that height ZINST. If the appropriate value of $\overline{U}\overline{\rho_g}/F$ is known, measurements of $\overline{U}$ and $\overline{\rho_g}$ at only that height are sufficient to calculate F. Wilson *et al.* (1982) give nomograms for circular plots of 20 and 50 m radius which first allow ZINST to be specified from knowledge of plot radius and surface roughness, and then permit the determination of the normalizing factor $(\overline{U}\overline{\rho_g}/F)$. Denmead (1983) and Wilson *et al.* (1983) give additional values for plots of 25 and 30 m radius.

Independent, empirical evidence for the existence of a ZINST is provided by figure 1 which illustrates the effects of atmospheric stability on the shape of the concentration profile. Although quite different in shape, the stable, unstable and neutral profiles all intersect within a narrow height range whose mid-point is about 0.8 m. The same behaviour can be expected for the horizontal flux density. Denmead (1983) provides further experimental evidence concerning ZINST, including that presented in figure 3, which was obtained in measurements of ammonia diffusion from urea-treated circular plots of short grass with a radius of 25 m. The figure shows plots of $\overline{U}\overline{\rho_g}$ at three different heights above the plot centre against the surface flux density F calculated from (2.2). It distinguishes between measurements made at night when stable conditions prevailed and those made during the daytime when conditions were mostly unstable. Lines of best fit which pass through the origin were calculated for the night-time and daytime observations at each height. The influences of stability on profile shape manifested in figure 1 are again evident: near the surface, at $z - d = 0.15$ m (d is the zero-plane displacement), the ratio of $\overline{U}\overline{\rho_g}$ to F is clearly higher in stable conditions than in unstable conditions, while in the top of the profile at 1.55 m, the reverse is true. At 0.75 m, the scatter is much reduced and the ratio is virtually independent of stability. Dividing the horizontal fluxes at that height by the slope of the line of best fit to the data (11.3) gives the surface flux F in all stability conditions with very small error.

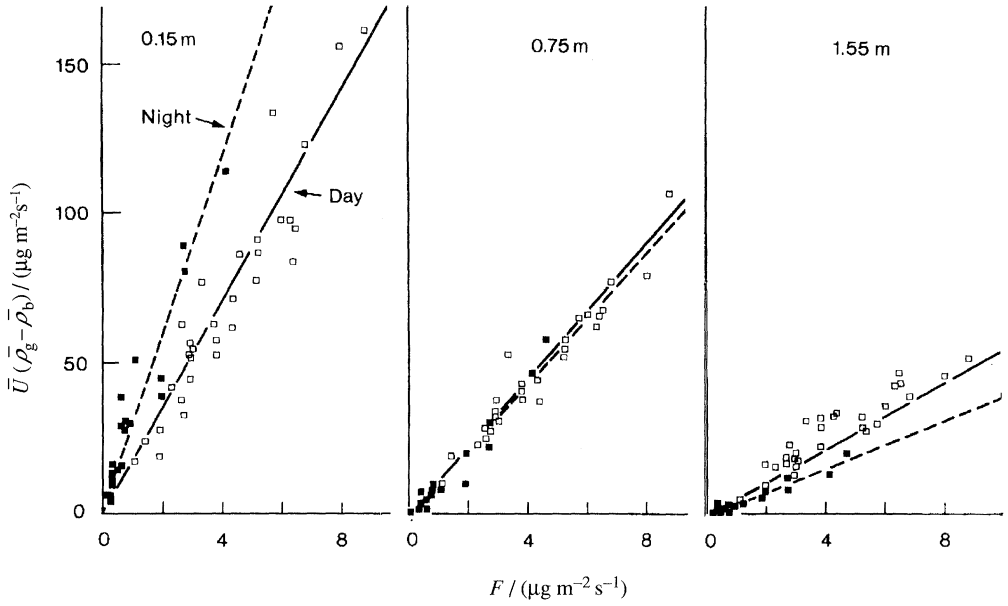

Figure 3. Relationship between horizontal flux density of ammonia at three heights ($\overline{U}\overline{\rho_g}$) and surface flux density (F) in urea-treated plots of short grass. Fetch over plot 25 m. Points are 2 h averages: open squares and solid lines for day time observations; solid squares and dashed lines for night time. Lines of best fit pass through the origin. (From Denmead 1983.)

(*c*) *Point sources*

The general mass balance method outlined above, but using full profiles of $\overline{U}$ and $\overline{\rho_g}$, has been used for measuring emissions of ammonia and methane from grassland during periods of grazing by cattle and sheep (Jarvis *et al.* 1989, 1993). A difficulty, in the case of methane at least, is that a good part of the gas production is directly from the animals which constitute moving point sources that may not necessarily be upwind of the central measuring point. A variant of the mass balance approach that overcomes this problem has been used recently by the author and colleagues, L. A. Harper and J. R. Freney, to measure CH_4 production by grazing cattle. In that instance, a complete methane budget was made for the field in which the animals were grazing.

Four cattle were grazed in a small field, 24 m×24 m. Sampling tubes were mounted at four levels along the complete length of each side. The CH_4 content of the air at each level was determined continuously by infrared gas analysis. Figure 4*a* shows example profiles of CH_4 concentrations on each of the two upwind and downwind boundaries. Wind speeds were measured at the same levels as the sampling tubes, along with wind direction, in order to calculate the flow of air across each boundary of the field, the U and V of figure 4*b*. The mean air flows during runs of 33 min were then combined with the mean concentration profiles to calculate first the horizontal flux profiles (figure 4*b*) and then the total fluxes of CH_4 across each boundary (figure 4*c*). The net efflux from the field (the sum of the S and E fluxes in figure 4*c* less the sum of the N and W fluxes) represented CH_4 production by the cattle.

The potential of the method for investigating emissions from isolated point sources or small intense land sources, is evidently very high. Other problems

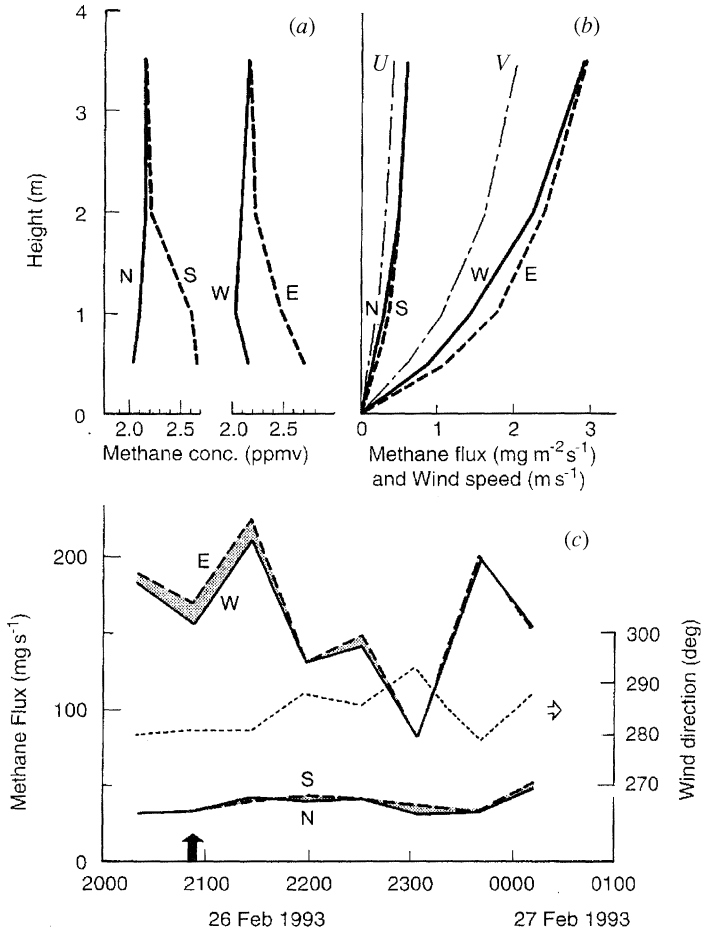

Figure 4. (*a*) Vertical profiles of CH_4 concentration on each boundary of experimental field for one experimental run with a NW wind. N, S, E, W denote compass points; solid lines for upwind profiles; dashed lines for downwind profiles. (*b*) Vector winds across N and S boundaries, denoted by U, and E and W boundaries, denoted by V, and corresponding CH_4 flux densities. (*c*) Wind direction and net CH_4 fluxes across each of the boundaries. Stippled area represents CH_4 production by the cattle. Arrow indicates time of the run in (*a*) and (*b*).

for which it could be exploited include CH_4 production from termite mounds, production of CH_4, CO_2, N_2O and toxic gases from landfills and dumps, and N_2O production during and after grazing.

3. Inverse Lagrangian techniques

The most comprehensive treatment of Lagrangian dispersion in the canopy space is contained in publications on the topic by M. R. Raupach, notably Raupach (1987, 1989*a*–*c*). Here it is possible to give only a rudimentary outline. A feature of Raupach's analysis is treatment of dispersion in separate regions near to and far from the source elements (foliage elements and the ground). Scalar concentration C within the canopy results from contributions C_n from the near

field and C_f from the far field. Thus

$$C(z) = C_n(z) + C_f(z), \tag{3.1}$$

where the subscripts n and f refer to the near and far fields. In the near field, dispersion is dominated by the local coherence of eddy motions. The near field region extends about one canopy height downwind of any particular source. Within this region, the size of the scalar cloud generated by a source element increases linearly with the time of liberation or travel, t. In the far field, dispersion is dominated by the randomness of the turbulence and the cloud size grows approximately as $t^{1/2}$. The dispersion process in the far field can be described by turbulent diffusion along the mean concentration gradient.

The near field concentration is obtained from knowledge of the source strength S and the turbulence, as characterized by σ_w, the standard deviation of the vertical wind speed w and T_L, the Lagrangian time scale for vertical velocity, which is a measure of the average persistence time of eddies. Designating the height of a particular source element by z_0,

$$C_n(z) = \int_0^\infty \frac{S(z_0)}{\sigma_w z_0} \left\{ k_n \left[\frac{z - z_0}{\sigma_w(z_0) T_L(z_0)} \right] + k_n \left[\frac{z + z_0}{\sigma_w(z_0) T_L(z_0)} \right] \right\} \mathrm{d}z_0, \tag{3.2}$$

where k_n is a near field kernel derived and tabulated in Raupach (1989*a*). The parameter σ_w is a datum of the problem and in practical applications to date, T_L is obtained empirically from u_*. In the applications described here,

$$T_L(z) u_*/h = \max[c_0, k(z - d)/a_1 h], \tag{3.3}$$

where h is canopy height, u_* is the friction velocity, c_0 is an empirical constant (set equal to 0.3), k is von Karman's constant, d is the zero-plane displacement and $a_1 = \sigma_w(z)/u_*$.

The far field concentration component is obtained by solution of the turbulent diffusion equation,

$$F_z = -K_z \partial C_f / \partial z, \tag{3.4}$$

where K_z, the far field eddy diffusivity, is

$$K_z = \sigma_w^2 T_L(z). \tag{3.5}$$

Through these equations, Raupach (1989*b*) relates concentration at any level i ($i = 1$ to n) to the source strengths at all levels j ($j = 1$ to m) using a dispersion matrix D with elements D_{ij}:

$$C_i - C_R = \sum_{j=1}^{m} D_{ij} S_j \Delta z_j, \tag{3.6}$$

where C_R is the concentration at a reference level above the canopy, m represents the number of discrete source layers, each with strength S_j, and Δz_j is the depth of source layer j. The elements D_{ij} are calculated from the statistics of the turbulence (u_*, σ_w, T_L) through procedures described in Raupach (1989*a*, *b*).

Equation (3.6) is the solution to the forward problem, namely predicting concentrations from source strengths. Raupach (1989*b*) extends the Lagrangian analysis to the inverse problem, that of determining source strengths from the concentrations. In that paper, he recommends that to ensure a stable solution for

PHILOSOPHICAL TRANSACTIONS OF THE ROYAL SOCIETY A MATHEMATICAL, PHYSICAL & ENGINEERING SCIENCES

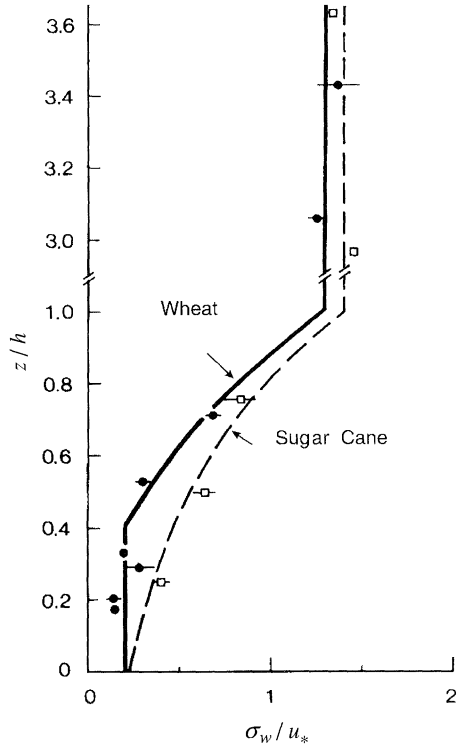

Figure 5. Measured profiles of σ_w/u_* (where u_* is the friction velocity above the crop) in the canopies of wheat (dots) and sugar cane crops (squares).

the source profile S_j, redundant concentration data should be included, so that source densities, S_j, in m layers are sought with n measured concentration values, $\hat{C}_i$, with $n > m$. He goes on to describe a best-fit, least-squares procedure for obtaining the S_{ij}.

(*a*) *Applications*

Raupach (1989*b*) tested his procedure for calculating S from C by analysing data on the dispersion of heat from an elevated plane source in a wind tunnel canopy. More recently, Raupach *et al.* (1992) have applied the inverse Lagrangian model to the problem of inferring sources and sinks of water vapour and CO_2 in the canopy of a wheat crop. This last analysis is now extended to an examination of changing seasonal patterns of CO_2 exchange in the same wheat crop, and to studies of heat and water vapour transport in the canopy of a crop of sugar cane. Because of contrasting geometries, the two crops provide a stringent test of the appropriateness of the near-field/far-field description of canopy transport. The wheat crop was dense with a maximum green leaf area index of 3 and a separation of 17.5 cm between the rows. The sugar cane crop was a ratoon crop with a leaf area index of 1.5 and 1.5 m between the rows. In both cases, concentration measurements were made at eight heights (two above and six within the canopy) and the number of source layers was set at four.

Figure 5 shows normalized profiles of σ_w obtained with sonic anemometers in each crop. The best-fit relationships shown in figure 5 were used to calculate σ_w in individual experimental runs from measurements of u_* above the crop.

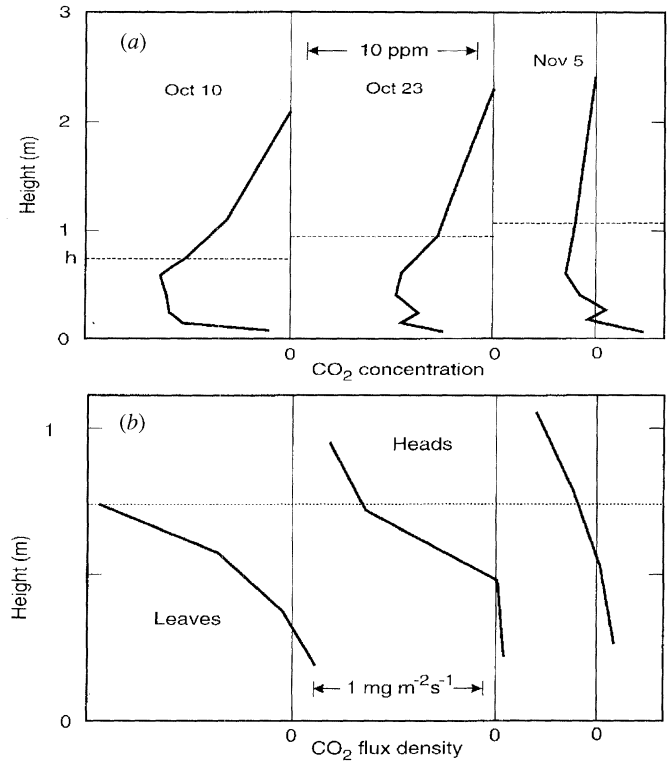

Figure 6. (*a*) Profiles of atmospheric CO_2 concentration within and above the canopy of a wheat crop measured near midday at two-week intervals covering reproductive development and senescence. (*b*) Corresponding profiles of the CO_2 flux density in the canopy as determined by inverse Lagrangian analysis.

As expected, the turbulence was extinguished much more rapidly with height in the dense wheat canopy. At mid-canopy, σ_w/u_* was only half as much in the wheat crop as in sugar cane. Figure 6 shows a sequence of near-midday CO_2 concentration profiles and the corresponding CO_2 fluxes calculated by the inverse Lagrangian method in the canopy of the wheat crop, as the crop advanced from the vegetative stage to near maturity over four weeks (figure 6*a*, *b*, respectively). Notable features are the early dominance of CO_2 assimilation by the mid-canopy foliage and its later dominance by CO_2 assimilation in the ears.

Figure 7 examines the credibility of the Lagrangian inferences by comparing scalar fluxes at the top of the canopy predicted by the analysis, i.e. $\sum_j S_j \Delta z_j$, with fluxes measured in the air layer above the crop by conventional micrometeorological approaches.

Figure 7*a* shows excellent agreement between the fluxes of CO_2 to the wheat crop predicted by the analysis and measured by eddy correlation. Figures 7*b* and 7*c* indicate similarly good agreement between predicted and observed fluxes for the sugar cane crop. Figure 7*b* compares the inverse Lagrangian prediction of the total flux of sensible heat from the crop to the atmosphere with measurements via eddy correlation and the energy balance. Figure 7*c* does the same for water vapour. The predictions agree as well with the means of the two micrometeorological measurements as these agree with each other.

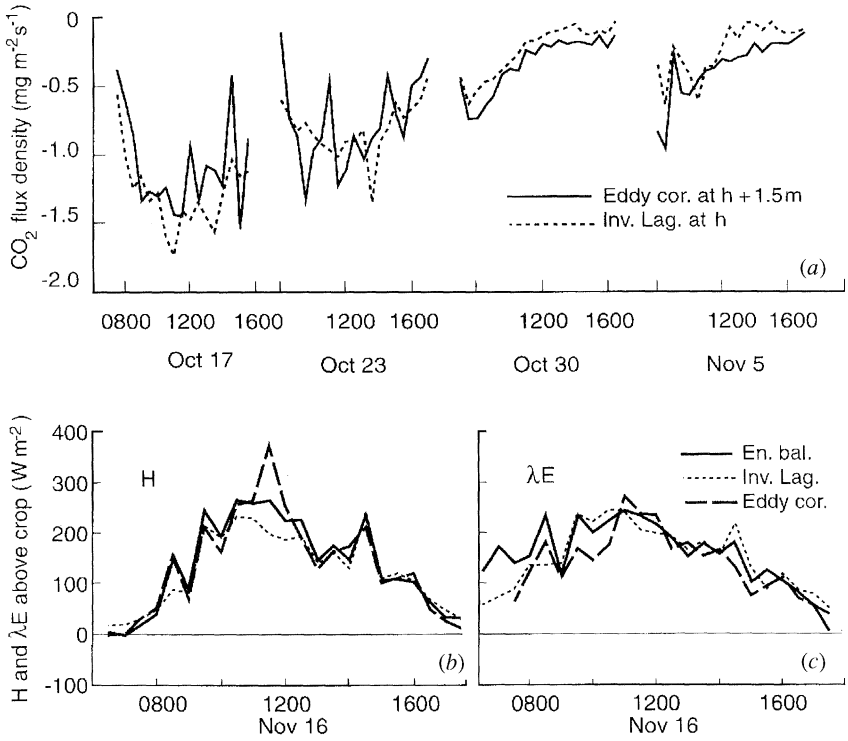

Figure 7. (*a*) Predictions by the inverse Lagrangian model of CO_2 fluxes at the top of the canopy of a wheat crop (h) and direct determinations of the CO_2 fluxes by eddy correlation at $h+1.5$ m. (*b*) Predictions by an inverse Lagrangian model of sensible heat flux at the top of a sugar cane crop (h) and direct measurements of the sensible heat flux (H) from the canopy by the energy balance and by eddy correlation. (*c*) Ditto for latent heat.

Both investigations indicate that the inverse Lagrangian approach is a very useful tool for calculating source–sink distributions in plant canopies. The apparent success of the method in dense and open crops and for different scalars is particularly encouraging. None the less, some problems still remain. These include the influence of thermal stratification on transport processes in the canopy and a rigorous description of turbulent transfer at the ground, where the present model is probably weakest.

I am grateful to my colleagues, F. X. Dunin, L. A. Harper, J. R. Freney and R. Leuning for permission to use unpublished data we have obtained. I also acknowledge the contribution of Michael Raupach, who has assisted me greatly in understanding and using his inverse Lagrangian technique.

References

Beauchamp, E. G., Kidd, G. E. & Thurtell, G. 1978 Ammonia volatilization from sewage sludge applied in the field. *J. Environ. Qual.* **7**, 141–146.

Collineau, S. & Brunet, Y. 1993 Detection of coherent motions in a forest canopy. I. Wavelet analysis. *Boundary-Layer Meteorol.* **65**, 357–379.

Denmead, O. T. 1983 Micrometeorological methods for measuring gaseous losses of nitrogen in the field. In *Gaseous loss of nitrogen from plant–soil systems* (ed. J. R. Freney & J. R. Simpson), pp. 133–157. The Hague: Martinus Nijhoff and Dr W. Junk.

PHILOSOPHICAL TRANSACTIONS OF THE ROYAL SOCIETY A MATHEMATICAL, PHYSICAL & ENGINEERING SCIENCES

Denmead, O. T. 1994 Measuring fluxes of CH_4 and N_2O between agricultural systems and the atmosphere. In CH_4 *and* N_2O *global emissions and controls from rice fields and other agricultural and industrial sources* (ed. K. Minami, A. Mosier & R. Sass), pp. 209–234. National Institute of Agro-Environmental Sciences, Tsukuba, Japan.

Denmead, O. T. & Bradley, E. F. 1985 Flux-gradient relationships in a forest canopy. In *The forest–atmosphere interaction* (ed. B. A. Hutchinson & B. B. Hicks), pp. 421–442. Dordrecht: Reidel.

Denmead, O. T. & Bradley, E. F. 1987 On scalar transport in plant canopies. *Irrig. Sci.* **8**, 131–149.

Denmead, O. T. & Raupach, M. R. 1993 Methods for measuring atmospheric gas transport in agricultural and forest systems. In *Agricultural ecosystem effects on trace gases and global climate change* (ed. L. A. Harper *et al.*), pp. 19–43. ASA Spec. Publ. 55. Madison: ASA, CSSA and SSSA.

Finnigan, J. J. 1979 Turbulence in waving wheat. II. Structure of momentum. *Boundary-Layer Meteorol.* **16**, 213–236.

Finnigan, J. J. & Raupach, M. R. 1987 Transfer processes in plant canopies in relation to stomatal characteristics. In *Stomatal function* (ed. E. Zeiger, G. D. Farquhar & I. R. Cowan), pp. 385–429. Stanford University Press.

Freney, J. R., Denmead, O. T., Wood, A. W., Saffigna, P. G., Chapman, L. S., Ham, G. J., Hurney, A. P. & Stewart, R. L. 1992 Factors controlling ammonia loss from trash covered sugar cane fields fertilised with urea. *Fert. Res.* **31**, 341–353.

Jarvis, S. C. 1990 Nutrient flows and transfers. In *ARFC Institute of Grassland and Environmental Research Report for 1990*, pp. 48–56. Hurley, U.K.

Jarvis, S. C., Hatch, D. J. & Roberts, D. H. 1989 The effects of grassland management on nitrogen losses from grazed swards through ammonia volatilization: the relationship to excretal N returns from cattle. *J. Agric. Sci. Camb.* **112**, 205–216.

Jarvis, S. C., Hatch, D. J. & Dollard, G. J. 1993 Greenhouse gas exchanges with temperate grassland systems. In *Proc. 17th Int. Grassland Congr. 1993*, pp. 1197–1198.

Leclerc, M. Y. & Thurtell, G. W. 1990 Footprint prediction of scalar fluxes using a Markovian analysis. *Boundary-Layer Meteorol.* **52**, 247–258.

Leuning, R., Freney, J. R., Denmead, O. T. & Simpson, J. R. 1985 A sampler for measuring atmospheric ammonia flux. *Atmos. Environ.* **119**, 1117–1124.

Raupach, M. R. 1987 A Lagrangian analysis of scalar transfer in vegetation canopies. *Q. Jl R. Meteorol. Soc.* **113**, 107–120.

Raupach, M. R. 1989*a* A practical Lagrangian method for relating scalar concentrations to source distributions in vegetation canopies. *Q. Jl R. Meteorol. Soc.* **115**, 609–632.

Raupach, M. R. 1989*b* Applying Lagrangian fluid mechanics to infer scalar source distributions from concentration profiles in plant canopies. *Agric. For. Meteorol.* **47**, 85–108.

Raupach, M. R. 1989*c* Stand overstorey processes. *Phil. Trans. R. Soc. Lond.* B **324**, 175–190.

Raupach, M. R., Coppin, P. A. & Legg, B. J. 1986 Experiments on scalar dispersion within a model canopy. I. The turbulence structure. *Boundary-Layer Meteorol.* **35**, 21–52.

Raupach, M. R., Denmead, O. T. & Dunin, F. X. 1992 Challenges in linking atmospheric CO_2 concentrations to fluxes at local and regional scales. *Aust. J. Bot.* **40**, 697–716.

Raupach, M. R. & Legg, B. J. 1984 The uses and limitations of flux-gradient relationships in micrometeorology. *Agric. Water Manag.* **8**, 119–131.

Ryden, J. C. & McNeill, J. E. 1984 Application of the micrometeorological mass balance method to the determination of ammonia loss from a grazed sward. *J. Sci. Food Agric.* **35**, 1297–1310.

Schoerring, J. K., Sommer, S. G. & Ferm, M. 1992 A simple passive sampler for measuring ammonia emission in the field. *Water Air Soil Pollut.* **62**, 13–24.

Shaw, R. H., Tavengar, J. & Ward, D. P. 1983 Structure of the Reynolds stress in a canopy layer. *J. Clim. Appl. Meteorol.* **22**, 1922–1931.

Shaw, R. H. & Schumann, U. 1992 Large-eddy simulation of turbulent flow above and within a forest. *Boundary-Layer Meteorol.* **61**, 47–64.

PHILOSOPHICAL TRANSACTIONS OF THE ROYAL SOCIETY A MATHEMATICAL, PHYSICAL & ENGINEERING SCIENCES

Wilson, J. D., Catchpoole, V. R., Denmead, O. T. & Thurtell, G. W. 1983 Verification of a simple micrometeorological method for estimating the rate of gaseous mass transfer from the ground to the atmosphere. *Agric. Meteorol.* **29**, 183–189.

Wilson, J. D. & Shaw, R. H. 1977 A higher order closure model for canopy flow. *J. appl. Meteorol.* **16**, 1197–1205.

Wilson, J. D. & Shum, W. K. N. 1992 A re-examination of the integrated horizontal flux method for measuring volatilisation from circular plots. *Agric. For. Meteorol.* **57**, 281–295.

Wilson, J. D., Thurtell, G. W., Kidd, G. E. & Beauchamp, E. G. 1982 Estimation of the rate of gaseous mass transfer from a surface plot to the atmosphere. *Atmos. Environ.* **16**, 1861–1867.

PHILOSOPHICAL TRANSACTIONS OF THE ROYAL SOCIETY A MATHEMATICAL, PHYSICAL & ENGINEERING SCIENCES